

Minerva Access is the Institutional Repository of The University of Melbourne

Author/s:

Hoppe, U;Brademann, G;Stöver, T;Ramos De Miguel, A;Cowan, R;Manrique, M;Falcón-González, JC;Hey, M;Baumann, U;Huarte, A;Liebscher, T;Bennett, C;English, R;Neben, N;Ramos Macías, A

Title:

Evaluation of a Transimpedance Matrix Algorithm to Detect Anomalous Cochlear Implant Electrode Position

Date:

2022-09-01

Citation:

Hoppe, U., Brademann, G., Stöver, T., Ramos De Miguel, A., Cowan, R., Manrique, M., Falcón-González, J. C., Hey, M., Baumann, U., Huarte, A., Liebscher, T., Bennett, C., English, R., Neben, N. & Ramos Macías, A. (2022). Evaluation of a Transimpedance Matrix Algorithm to Detect Anomalous Cochlear Implant Electrode Position. *Audiology and Neurotology*, 27 (5), pp.347-355. <https://doi.org/10.1159/000523784>.

Persistent Link:

<https://hdl.handle.net/11343/309001>

License:

[CC BY-NC](#)

# Evaluation of a Transimpedance Matrix Algorithm to Detect Anomalous Cochlear Implant Electrode Position

Ulrich Hoppe<sup>a</sup> Goetz Brademann<sup>b</sup> Timo Stöver<sup>c</sup> Angel Ramos de Miguel<sup>d</sup>  
Robert Cowan<sup>e</sup> Manuel Manrique<sup>f</sup> Juan Carlos Falcón-González<sup>d</sup>  
Matthias Hey<sup>g</sup> Uwe Baumann<sup>h</sup> Alicia Huarte<sup>i</sup> Tim Liebscher<sup>a</sup>  
Christopher Bennett<sup>j</sup> Ruth English<sup>k</sup> Nicole Neben<sup>l</sup> Angel Ramos Macías<sup>m</sup>

<sup>a</sup>Audiology, Universitätsklinikum Erlangen, Erlangen, Germany; <sup>b</sup>Otorhinolaryngology – Head and Neck Surgery, UKSH Kiel, Kiel, Germany; <sup>c</sup>Otorhinolaryngology – Head and Neck Surgery, Klinikum der J.W. Goethe-Universität, Frankfurt, Germany; <sup>d</sup>Acoustic Lab – Audiology, Complejo Hospitalario Universitario Insular Materno-Infantil de Gran Canaria, Las Palmas, Spain; <sup>e</sup>HEARing CRC, University of Melbourne, Melbourne, VIC, Australia; <sup>f</sup>Otorhinolaryngology – Head and Neck Surgery, Clínica Universidad de Navarra, Pamplona, Spain; <sup>g</sup>Audiology, UKSH Kiel, Kiel, Germany; <sup>h</sup>Audiology, Klinikum der J.W. Goethe-Universität, Frankfurt, Germany; <sup>i</sup>Audiology, Clínica Universidad de Navarra, Pamplona, Spain; <sup>j</sup>Algorithms and Applications, Cochlear Ltd., Macquarie University, Sydney, NSW, Australia; <sup>k</sup>Clinical Research, Cochlear Ltd., Melbourne, VIC, Australia; <sup>l</sup>Research and Science, Cochlear Deutschland GmbH & Co. KG, Hannover, Germany; <sup>m</sup>Otorhinolaryngology – Head and Neck Surgery, Complejo Hospitalario Universitario Insular Materno-Infantil de Gran Canaria, Las Palmas, Spain

## Keywords

Impedance · Cochlear implant · Surgical complications · Intraoperative monitoring · Electrical stimulation · Objective measures

## Abstract

**Introduction:** Transimpedance measurements from cochlear implant electrodes have the potential to identify anomalous electrode array placement, such as tip fold-over (TFO) or fold-back, basal electrode kinking, or buckling. Analysing transimpedance may thus replace intraoperative or post-operative radiological imaging to detect any potential misplacements. A transimpedance algorithm was previously developed to detect deviations from a normal electrode position with the aim of intraoperatively detecting TFO. The

algorithm had been calibrated on 35 forced, tip folded electrode arrays in six temporal bones to determine the threshold criterion required to achieve a sensitivity of 100%. Our primary objective here was to estimate the specificity of this TFO algorithm in patients, in a prospective study, for a series of electrode arrays shown to be normally inserted by post-operative imaging. **Methods:** Intracochlear voltages were intraoperatively recorded for 157 ears, using Cochlear's Custom Sound™ EP 5 electrophysiological software (Cochlear Ltd., Sydney, NSW, Australia), for both Nucleus® CI512 and CI532 electrode arrays. The algorithm analysed the recorded 22 × 22 transimpedance matrix (TIM) and results were displayed as a heatmap intraoperatively, only visible to the technician in the operating theatre. After all clinical data were collected, the algorithm was evaluated on the bench. The algorithm measures the transimpedance gradients and

corresponding phase angles ( $\theta$ ) throughout the TIM and calculates the gradient phase range. If this was greater than the predetermined threshold, the algorithm classified the electrode array insertion as having a TFO. **Results:** Five ears had no intraoperative TIM and four anomalous matrices were identified from heatmaps and removed from the specificity analysis. Using the 148 remaining data sets ( $n = 103$  CI532 and  $n = 45$  CI512), the algorithm had an average specificity of 98.6% (95.80%–99.75%). **Conclusion:** The algorithm was found to be an effective screening tool for the identification of TFOs. Its specificity was within acceptable levels and resulted in a positive predictive value of 76%, with an estimated incidence of fold-over of 4% in perimodiolar arrays. This would mean 3 out of 4 cases flagged as a fold-over would be correctly identified by the algorithm, with the other being a false positive. The measurements were applied easily in theatre allowing it to be used as a routine clinical tool for confirming correct electrode placement.

© 2022 The Author(s).  
Published by S. Karger AG, Basel

## Introduction

Cochlear implantation is a surgical procedure where an electrode array is inserted into the cochlea, either via a cochleostomy or the round window. The overall rate of complications during cochlear implant surgery is low, at around 5%–6%, and a significant proportion of these are the result of device failures or suboptimal electrode placement [Ishiyama et al., 2020]. Electrode positioning anomalies such as electrode kinking, partial insertion and tip fold-over (TFO) can be difficult to identify at the time of surgery, resulting in many going undetected until problems become apparent, e.g., poor performance or facial nerve stimulation [Zuniga et al., 2017]. Sometimes, switching off the affected electrode contacts can resolve the problems, but often patients must return to theatre, for revision surgery, to reposition the array.

TFOs occur when the apical tip of the electrode array does not advance into the cochlea as the array is inserted, but folds over or back on itself (Fig. 1a, b). Fold-over rates are low and have been reported to occur in less than 2% of implantations overall, but the problem is more prevalent in perimodiolar electrode arrays [Gabielpillai et al., 2018; Jwair et al., 2021]. There is often no surgical awareness from the feel, and detection requires objective imaging to confirm [Dimak et al., 2020]. In an ideal world, no patient should leave theatre with a misplaced electrode array, and thus, it is essential to find a method of providing an accurate estimate of electrodeposition intraoperatively. Objec-

tive radiological imaging is the gold standard for identifying electrodeposition, but this requires additional equipment, time in theatre, expense, and radiation exposure of the patient. Techniques such as a modified Stenvers X-ray do not always detect TFO and even CT imaging can be poor as a result of blurring of the electrode contacts due to artefacts (e.g., Fig. 1a, lower) [Gabielpillai et al., 2018].

An alternative quality control method is to use the electrophysiological profile of the electrode array and the back telemetry facility of current CI devices to infer device shape [Vanpoucke et al., 2012]. Techniques such as measuring the spread of excitation of the neural response or the intracochlear potential profile can provide an indication of the device's shape without the need for imaging [Grolman et al., 2009; Zuniga et al., 2017]. These methods can easily be used intraoperatively, allowing any electrode placement issues to be corrected without the need for a second surgery.

Vanpoucke et al. [2012] described a method of using electric field imaging to create an electrical distance matrix from differences in the passive voltage measured at adjacent recording electrodes [Vanpoucke et al., 2012]. The voltages measured at each recording electrode are normalized, by dividing by stimulating current, to produce impedance values (Ohm's Law) or "transimpedances." Following Gauss's and Coulomb's laws, transimpedance ( $R$ ) varies according to the distance between stimulating and recording contacts  $r$ , parameters of the electrode-medium interface  $T$ , and the permittivity of the medium  $k\epsilon_0$  (Eq. (1)).

$$R = \frac{1}{r} \times \frac{T}{4\pi k\epsilon_0}. \quad (1)$$

The values of  $T$  and  $k\epsilon_0$  remain largely constant across the array; therefore, much of the variation in  $R$  is inversely proportional to the distance  $r$  between stimulating and recording contacts. A standard Cochlear (Cochlear Ltd., Sydney, NSW, Australia) electrode array has 22 electrode contacts and a  $22 \times 22$  matrix can be created from the transimpedances recorded at each electrode, as each electrode is stimulated in turn. The transimpedances can then be displayed as a heatmap (Fig. 1c, d). Klabbers et al. [2021] described how intraoperative transimpedance matrix (TIM) measures, displayed as a heatmap, could be used clinically to correctly identify TFOs [Klabbers et al., 2021]. Alternatively, multidimensional scaling can be applied to determine the configuration of the electrode array, as shown in Figure 1e, f, illustrating the spatial information coded in the TIM data [de Leeuw and Mair, 2009; Vanpoucke et al., 2012].

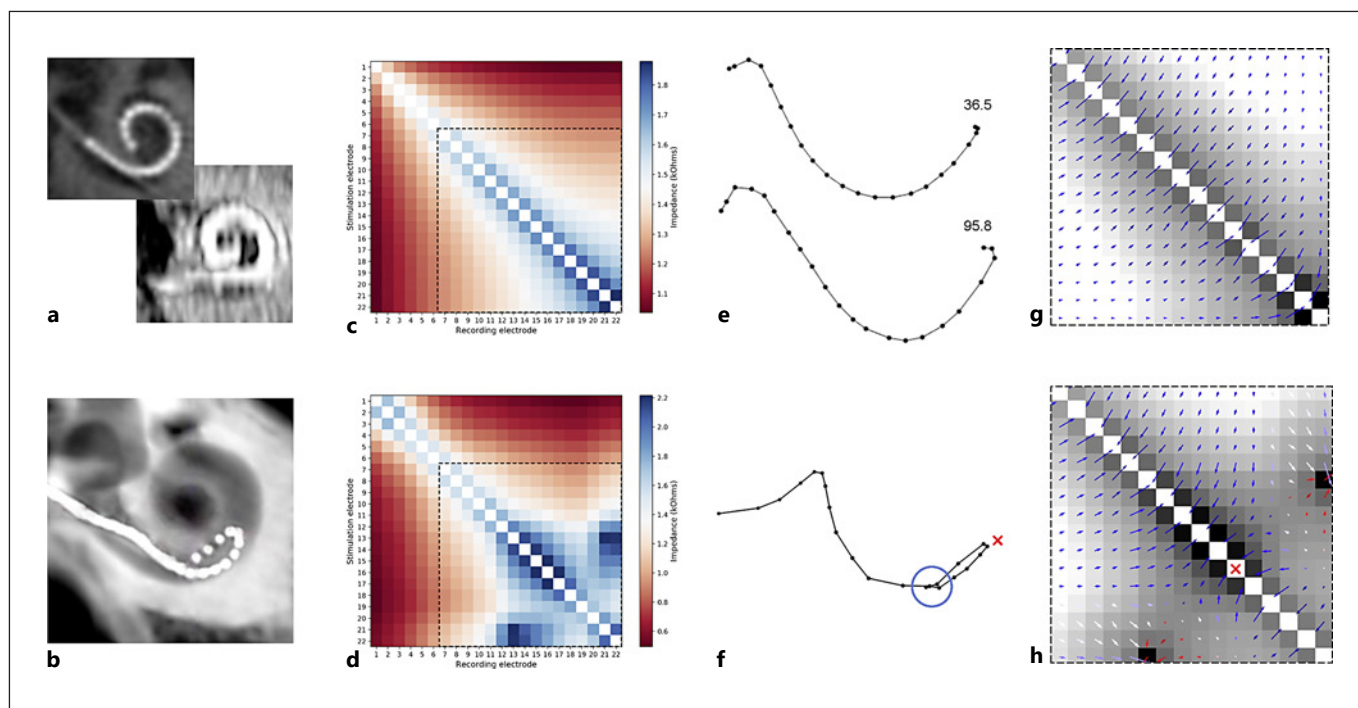


**Fig. 1.** Representations of well-positioned electrode arrays in the upper row and with TFO in lower row. **a** High-resolution clinical CT images can be of inconsistent quality. **b** CT image of ex vivo temporal bone with TFO. **c, d** TIM heatmaps. High off-axis impedances in the heat map can indicate a TFO. **e** Spatial configurations of electrode contacts obtained from applying metric MDS to in-

verted transimpedance data, for example, with gradient phase range  $36.5^\circ$  and  $95.8^\circ$ . **f** Similar MDS configuration showing electrodes brought close (blue circle) together due to a fold (red  $\times$ ). **g, h** Enlarged images of heatmaps in **c** and **d** with arrows to indicating gradient phase vectors. The red arrows indicate areas where the gradient phases are atypical. MDS, multidimensional scaling.

A TFO detection algorithm using transimpedance measurements was developed by Cochlear to detect deviations from normal electrodeposition. Normally, the electrode array either sits smoothly, along the lateral wall of the scala tympani for a straight array or, along the modiolar wall for a perimodiolar array. A TFO moves the electrode array, or at least portions of it, away from its expected “normal position” within the cochlea and leaves the point of deepest insertion shallower than for normal position (Fig. 1b vs. 1a, 1f vs. 1e) which might affect performance or sound quality. The sensitivity of the algorithm was previously validated in an unpublished temporal bone study (i.e., the number of true positive responses recorded by the test divided by the total number of positive cases). Due to the low incidence of TFO, testing the sensitivity of the algorithm in patients was not considered viable. In the study, a TFO was generated in human temporal bones, confirmed using CT imaging, and then transimpedance measurements were recorded. Data were analysed from 35 Nucleus<sup>®</sup> CI532 electrode arrays, inserted into six temporal bones. A sensitivity of 100% (90% con-

fidence interval 92–100%) was calculated using the Clopper-Pearson exact method. However, setting the parameters of the algorithm to achieve such a high sensitivity could result in a high number of false positives, i.e., low specificity, which is undesirable in a clinical tool, resulting in the unnecessary repositioning of electrode arrays.

The primary objective of the prospective clinical study described in this paper was to explore the specificity of the TFO algorithm in a clinical setting, in real patients, in a series of electrode arrays known to be normally inserted. The secondary objective was to establish a normal range of transimpedances and investigate the stability of the transimpedance measurements over time.

## Methods

### Subjects

Subjects aged 18 or over were enrolled across six investigational sites in Germany, Spain, and Australia and with 15 implanting surgeons. Bilateral subjects were assigned a separate subject number for each ear. All subjects had normal cochlea anatomy, estab-

**Table 1.** Evaluation schedule

Procedure	Pre-op	Surgery	First activation ±1 month	3 months post-op ±1 month
Informed consent	X			
Demographics, medical and hearing history	X			
Surgical questionnaire		X (after electrode insertion)		
TIM measures		X (after electrode insertion)	X	X
Radiological imaging	X	X (after electrode insertion, may be done after surgery)		

lished via preoperative CT/DVT scans, and received a Nucleus® CI532 or CI512 device. Subjects were excluded who had prior cochlear implantation in the ear to be implanted, ossification, or any other cochlear anomaly that might prevent complete insertion of the electrode array or additional handicaps that would prevent participation in evaluations.

#### Study Design

Data were collected prospectively with sequential enrolment. Measurements, including CT/DVT scans before and after surgery, were collected as part of the clinical routine test battery in participating centres. Adverse events were actively followed up. Data were collected using electronic forms filled in by the investigators in Medidata, a web-based system for electronic data capturing. The evaluation schedule is presented in Table 1.

#### Surgical Questionnaire

A surgical questionnaire was used to collect information on the surgical approach, electrodeposition, and insertion-related events. All surgeons made their own assessment of whether a TFO occurred during surgery based on their clinical routine method. This was documented by the surgeon in the surgical questionnaire. Any TFOs identified were either corrected at the time of surgery or during a follow-up procedure. Post-operative imaging was used for final confirmation of the absence of TFO (see below).

#### Transimpedance Measurements

Transimpedance matrices (TIMs) were measured using Custom Sound™ EP 5 programming software and a Nucleus® CP900 Series processor with a Nucleus® Programming Pod (Cochlear Ltd.). This system uses an automatic procedure to measure the intracochlear voltage, passively induced on each non-stimulated recording electrode, for each of the 22 stimulating electrodes in turn, based on the methods described in Vanpoucke et al. [2012]. Voltages were measured at the end of the first (cathodic) phase. An automated algorithm adjusted the current level until voltage compliance was obtained, and the measurement amplifier was not saturated, which typically resulted in measurements performed at 190–210 current level units. Stimulation is referenced to the ground electrode and values are normalized by the stimulating current used to produce a measure of transimpedance and a 22 × 22 matrix is created. The recordings took between 1 and 3 min to complete. Measurements made during surgery were used to test the TFO algorithm. Further measurements were made at activation and 3-month postoperatively.

#### Post-Operative Imaging

CT or DVT imaging was conducted during or immediately after surgery according to the routine protocol and available equipment in each participating clinic. A variety of flat-panel digital volume or rotational tomography (“ConeBeam”) systems were used. The following imaging parameters were recommended: 80–125 kV, 7–50 mA, with a 360° rotation of 18–40 s duration (pulsed). Projection images were obtained from a cylindrical volume of 7–8 cm in height, by 7–8 cm diameter for a single temporal bone or 12–15 cm diameter for both temporal bones.

#### TIM Analysis

TIMs from the normally inserted arrays were included in the specificity analysis. The intraoperative TIM heat maps were visually screened for completeness and checked for missing or abnormal values and any open and short-circuited electrodes, after study completion (Fig. 1c, d). The introduction of additional asymmetric anomalies may increase the likelihood of false positives or false negatives. Therefore, when a TIM with at least one anomalous feature was identified, TIM was removed from the analysis. Measurements affected by asymmetric anomalies were identified by an absolute difference between the TIM and its transpose of greater than 36 Ω, determined from the inherent noise in the measurement system. Due to the way in which the TIM is filled in with the impedance measurements, features of electro-physical phenomena, such as a TFO, are symmetrically represented across the main diagonal of the TIM heatmap. Asymmetries in the heatmap are not likely to be due to electro-physical phenomena but are more likely to be due to a failure to adequately record the impedance measurements.

Next, valid TIMs were analysed by the TFO detection algorithm. The algorithm first calculates the 2-dimensional gradients of the TIM, with a corresponding magnitude and direction for each point in the matrix (Fig. 1g, h). The direction of each gradient, or gradient phase ( $\Theta$ ), is defined relative to a nominal vector, which is orthogonal to and pointing towards the main diagonal. For normal insertions, transimpedance values decrease with distance from the main diagonal in the TIM, or distance from the stimulating electrode, and so the gradients generally point toward the main diagonal (Fig. 1g). With a TFO, the monotonic drop in transimpedance with distance is disrupted and local gradients point in other directions (Fig. 1h).

The gradient phases across the TIM of a folded electrode largely deviate from the nominal vector pointing towards the main diagonal. Thus, the TFO detection algorithm uses the overall range of gradient phases in either triangle of the TIM to discriminate between normal and folded electrodepositions. Gradient phase

**Table 2.** Demographics and other surgical details of the study sample

Mean age	58 years (range 19–88)			
Gender	51% female			
Aetiology	Unknown ( <i>n</i> = 98)	Genetic ( <i>n</i> = 12)	Other ( <i>n</i> = 38)	
Type of loss	Progressive ( <i>n</i> = 20)	Congenital with progression ( <i>n</i> = 20)		Sudden ( <i>n</i> = 108)
Device	CI512 ( <i>n</i> = 45)	CI532 ( <i>n</i> = 103)		
Surgical approach	Cochleostomy ( <i>n</i> = 22)	Extended round window ( <i>n</i> = 62)	Round window ( <i>n</i> = 63)	Cochleostomy and blind sac closure ( <i>n</i> = 1)
Side implanted	Left ( <i>n</i> = 76)	Right ( <i>n</i> = 72)		

ranges above and below a threshold are then respectively classified as positive and negative for a TFO.

During the development of the TFO detection algorithm, experimental trials on electrode array insertions in temporal bones, with and without TFOs, generated two distributions of the gradient phase range. A threshold was selected by careful consideration of the trade-offs between sensitivity and specificity and the low incidence of TFOs. Thus, in the clinical data set, a gradient phase range greater than this predetermined threshold would indicate a TFO.

#### Statistics

The binomial 90% two-tailed confidence interval for specificity was derived using the Clopper-Pearson Exact Method. A minimum sample size of 145 ears was required so that the lower bound of the two-tailed 90% confidence interval for specificity was 98%. A TFO rate of 4%, following a binomial distribution, was assumed.

For the secondary objective, establishing a normal range of transimpedances and investigating the stability of the transimpedance measurements over time, separate analyses were performed for the CI532 and CI512 implants. The stability of measurements over time was ascertained by analysing the differences between intraoperative and activation and activation and 3-month post-operative. Differences between measures at different study time points were calculated on an individual subject basis.

## Results

TIM data were recorded from 145 subjects and 148 ears. From the initial sample of 157 ears, 5 ears had no TIM data intraoperatively (four CI512 and one CI532). Results for a further 4 ears were screened out during the analysis because of the TIM data showing measurement abnormalities that could be indicative of open-circuited electrodes or spurious measurements (three CI512 and one CI532). Demographics and other study sample details are given in Table 2.

#### Surgical Results

Electrode reinsertion was required for 4 subjects (2.5% of 157 ears) due to TFO. In 1 case a backup device was

inserted, whereas in the other 3 cases the same electrode was repositioned. The surgeons reported that the TFOs had been corrected in all cases, which was confirmed by imaging. The TFOs that occurred were correctly identified in all 4 cases by applying the algorithm to TIM data collected prior to electrode repositioning.

#### TFO Algorithm Results

The TFO algorithm identified two samples with a gradient phase range greater than the predetermined threshold. Neither of these cases was identified as having a TFO on CT imaging. This gave an average specificity of 98.64% with a 90% confidence interval of 95.80–99.75%. The probability density function, derived from the Clopper-Pearson method, has a distribution upwardly skewed towards 100% with a 0% chance that the calculated specificity is below 93%.

Using the 98.64% specificity measured here, the 100% sensitivity established in temporal bones, and a prevalence of 4%, a positive predictive value of 76% (90% confidence interval 49–95%) was calculated. The negative predictive value ranges from 99.6% to 100%.

#### Transimpedances by Electrode Type

Distributions for transimpedance values are given in Figure 2 for stimulating electrode 8, illustrating the normal range of values that can be expected for each electrode type. The roll-off of transimpedances was more rapid towards the base (electrode 1) compared with towards the apex for all stimulating electrodes. Measurements for other stimulating electrodes gave approximately the same range of values. Transimpedances for the CI532 and CI512 arrays had similar ranges.

#### Stability over Time

For both implant types, the change in the TIM measurement distribution between intraoperative and activation and between activation and 3-month post-operative

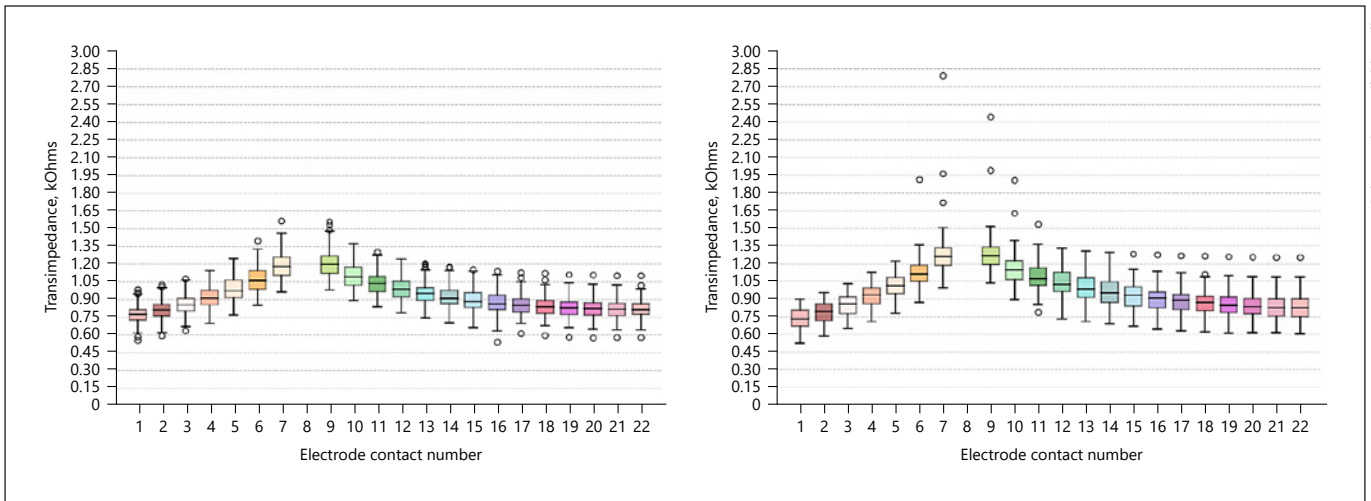


**Fig. 2.** Transimpedances measured intraoperatively for stimulation electrode 8 for the CI532 (left,  $n = 74$ ) and CI512 (right,  $n = 46$ ) arrays. These indicate the normal range of values that can be expected. Midlines are medians; boxes are quartiles; error bars are quartiles  $\pm 1.5$  interquartile range; points are outliers.

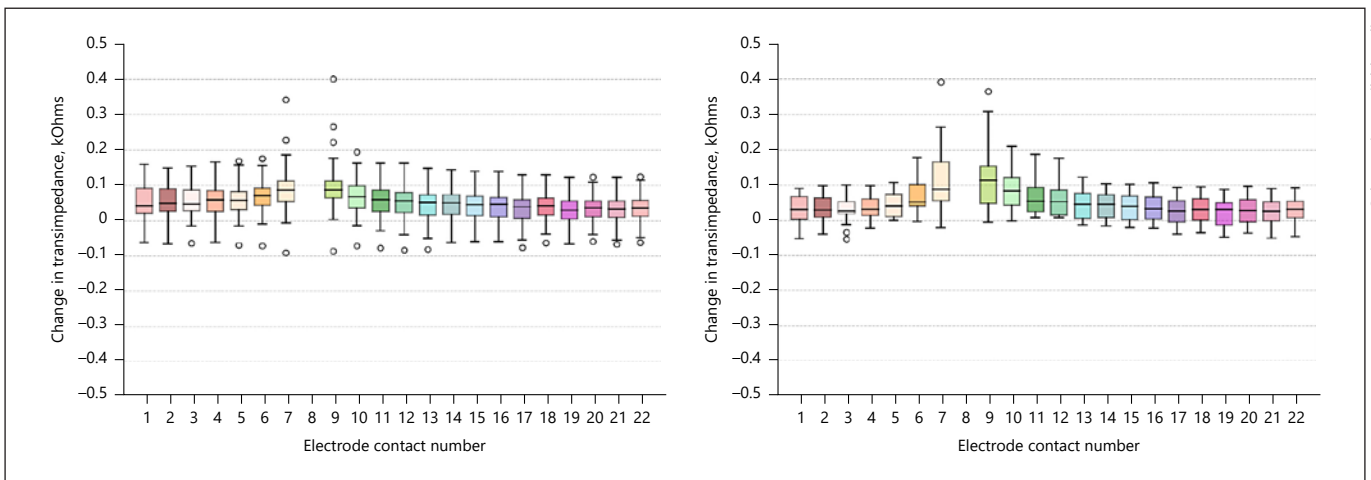


**Fig. 3.** The distribution of transimpedance changes between the intraoperative and activation time point for stimulating electrode 8 for CI532 (left,  $n = 43$ ) and CI512 (right,  $n = 16$ ). Changes were significant ( $p < 0.05$ ) between the intra-op and activation times, for recording electrodes 1–16 for the CI532, and for electrodes 4–10 for the CI512. Midlines are medians; boxes quartiles; error bars quartiles  $\pm 1.5$  interquartile range; points outliers.

follow-up showed a small general increase. Kruskal-Wallis tests were run on transimpedances per stimulating/recording electrode combination, with timepoint as the independent variable. Using stimulating electrode 8 as an example, there was a significant effect of timepoint on transimpedance across all recording electrodes (CI532:  $H > 27$ , all  $p < 0.001$ ; CI512:  $H > 11$ , all  $p < 0.005$ ) (Fig. 3). For CI532 devices, post hoc Dunn's tests revealed that

there was a significant increase in transimpedance between activation and the 3-month visit for all recording electrodes (all  $p < 0.001$ ). However, there was a significant increase between intra-op and activation for recording electrodes 1–16 ( $p < 0.05$ ). On the other hand, for CI512 devices, significant increases were seen between intra-op and activation for recording electrodes 4–10 ( $p < 0.05$ ), with no significant changes between activation and the

3-month visit. Transimpedance increases were small but statistically significant across all recording electrodes between intra-op and 3-month follow-up for both devices (all  $p < 0.0001$ ).

## Discussion

The cochlear implant TFO detection algorithm, we tested here, is an effective screening tool. The specificity of 98.6% was within acceptable levels and, with an estimated prevalence of TFO of 4% in perimodiolar arrays, resulted in a positive predictive value of 76%. This would mean 3 out of 4 cases flagged as a TFO would be correctly identified. The high negative predictive value of near 100% gives confidence that any array identified as not having a TFO is correctly inserted. The automated procedure enables the TIM measurements to be applied easily in theatre, which will allow it to be used as a routine clinical tool. We note that detecting asymmetries in the TIM caused by air bubbles or electrode faults can be trivially automated by comparing the values in the upper and lower triangles (Fig. 1c, d), eliminating the need to visually inspect the results.

The overall prevalence of TFO found in this study of 2.5% for the whole sample was in line with the 2% prevalence of TFO reported for all types of electrode arrays in a meta-analysis [Jwair et al., 2021]. However, due to the precurved nature and insertion technique required for perimodiolar arrays, these seem more susceptible to TFO [Gabielpillai et al., 2018; Jwair et al., 2021]. The results of our sample show a prevalence of 3.9% for TFO in the CI532 perimodiolar electrode array. This is lower than the prevalence of 5.9%, averaged across six studies with the CI532, reported by Jwair et al. [2021] but higher than the 1.8% reported by Hey et al. [2020]. Durakovic et al. [2020] reported TFO rates for CI532 ranging from 2% to 6%, with devices implanted more recently having lower rates [Durakovic et al., 2020]. Improvements to the CI532 sheath design in 2018, and increased surgeon experience with the insertion technique, have contributed to reduced incidence rates for more recently implanted devices.

Klabbers et al. [2021] showed that the concept of using TIMs to detect TFOs was viable, and other authors have shown that TIMs can also be used to detect extra-cochlear electrodes or to infer insertion depth [De Rijk et al., 2020; Aebischer et al., 2021; Klabbers et al., 2021]. However, this is the first test of a large-scale trial of a TFO tool as a replacement for routine intraoperative imaging. Using the TFO tool takes only a few minutes of surgery time

and does not require radiology to be on standby, unlike fluoroscopy and CT scanning. Equally importantly, it provides a low-cost method for identifying TFOs in clinics where intraoperative imaging is not available.

Other electrophysiological methods of deriving the electrode array position have been tried [Müller et al., 2021]. Neural response telemetry is one viable option but measuring the threshold of the evoked compound action potential was not found to be a reliable tool for detecting TFOs [Zuniga et al., 2017; Mittmann et al., 2020]. Using neural response telemetry to measure the spread of excitation, however, has produced some encouraging results [Grolman et al., 2009; Cosetti et al., 2012]. But this technique requires an experienced audiologist to interpret the results. Electrocochleography has also been experimented with but currently the available data are limited [Trecca et al., 2021].

It is a limitation of this study that the sensitivity could not be tested in a clinical sample. There is a low incidence of anomalous electrode position cases in normal clinical practice, and it is not ethical to experimentally generate anomalous electrode positions in subjects. Therefore, data from an earlier temporal bone study was used to show how effective the TFO algorithm was at detecting actual TFOs. The algorithm threshold was adjusted to be highly sensitive, but this may be at the expense of the specificity. However, its practical use as a screening tool in a clinical setting is to reduce the need for CT imaging in theatre, not to eliminate it entirely. Suspected TFOs will still require confirmation with CT imaging, but the need for CT scanning of all patients is reduced. Not missing any genuine TFOs is essential, thus sensitivity must be high. With the current settings, patients with a normal TIM can be confident that there is no TFO, but in 1 out of 4 cases where a TFO is flagged, it is incorrect. We consider this to be an acceptable rate of false positives and would still result in a significant reduction in the number of patients requiring intraoperative radiology specifically to exclude a TFO.

The TIM measures were largely stable with a small but statistically significant increase between the intraoperative and 3-month evaluation period for all recording electrodes and both devices. These were small enough not to be relevant and most likely reflect the known changes in impedance which occur after implantation due to fibrosis and inflammation around the array [Hey et al., 2019].

The 99% specificity measured here, and 100% sensitivity estimated from the temporal bone data, make this TFO algorithm a very suitable candidate as a screening tool to reduce the need for imaging in theatre purely for

the purpose of eliminating TFO as a complication. The number of implanting centres and surgeons, and the range of patients included provide confidence that the results should be applicable to all implant centres. Further study is required to establish the application of TIM to provide a reliable guide to identify other cochlear implant electrode placement anomalies. Future work using device telemetry is needed to establish intraoperative electrophysiological, voltage gradient, or impedance measures. This will establish the limitations of these approaches for confirming exact electrode array position within the cochlea. This in turn will have two benefits as follows: (1) to replace the need for intra or post-op imaging and (2) to ensure patients leave the operating theatre with confirmation of an optimally placed electrode array.

### Acknowledgments

We would like to thank Paula Greenham and Chris James for their help in writing the manuscript. Ryan Melman and Matt Zygorodimos of Cochlear Ltd. developed the TFO algorithm.

### Statement of Ethics

All subjects gave their informed written consent before taking part. Ethics approval was obtained from the respective Ethics Committees of each hospital involved and the study was completed in accordance with the principals laid out in the declaration of Helsinki (<https://www.wma.net/policies-post/wma-declaration-of-helsinki-ethical-principles-for-medical-research-involving-human-subjects/>). The respective Ethic Committees were Comité Ético Investigación Complejo Hospitalario Universitario Insular-Materno Infantil in Las Palmas, Spain (2018-202-1/944); Comité Ético Investigación Clínica de Navarra in Pamplona, Spain (EO17/15); Ethik-Kommission des Fachbereichs Medizin Univer-

sitätsklinikum der Goethe-Universität in Frankfurt, Germany (338/17); Ethik-Kommission der Medizinischen Fakultät der Christian-Albrechts-Universität zu Kiel in Kiel, Germany (D545/17); Ethik-Kommission der Medizinischen Fakultät Friedrich-Alexander-Universität Erlangen-Nürnberg in Erlangen, Germany (208\_17 B); and The Royal Victorian Eye and Ear Hospital Human Research Ethics Committee in Melbourne, Australia (18/1385H). The ClinicalTrials.gov identifier of this investigation is NCT03294681.

### Conflict of Interest Statement

Nicole Neben, Ruth English, and Christopher Bennett are employees of Cochlear, the sponsor of this investigation. Angel Ramos Macías is now Editor-in-Chief of the journal. The other authors have no conflicts of interest to declare.

### Funding Sources

Cochlear Ltd., the manufacturer of Nucleus cochlear implant systems, sponsored the study.

### Author Contributions

A.R. de M., A.R.M., and N.N. conceived and designed the study and contributed to the report. N.N. managed the study on behalf of the sponsor. C.B. performed the statistical analysis and wrote together with R.E. the clinical investigation report. All authors guaranteed the data and approved the manuscript.

### Data Availability Statement

The data that support the findings of this study are available from the study sponsor, upon reasonable request.

### References

- Aebischer P, Meyer S, Caversaccio M, Wimmer W. Intraoperative impedance-based estimation of cochlear implant electrode array insertion depth. *IEEE Trans Biomed Eng*. 2021;68:545–55.
- Cosetti MK, Troob SH, Latzman JM, Shapiro WH, Roland JT, Waltzman SB. An evidence-based algorithm for intraoperative monitoring during cochlear implantation. *Otol Neurotol*. 2012;33:169–76.
- De Rijk SR, Tam YC, Carlyon RP, Bance ML. Detection of extracochlear electrodes in cochlear implants with electric field imaging/transimpedance measurements: a human cadaver study. *Ear Hear*. 2020;41(5):1196–207.
- Dimak B, Nagy R, Perenyi A, Jarabin JA, Schulcz R, Csanady M, et al. Review of electrode placement with the slim modiolar electrode: identification and management. *Ideggyogy Sz*. 2020;73:53–9.
- Durakovic N, Kallogjeri D, Wick CC, McJunkin JL, Buchman CA, Herzog J. Immediate and 1-year outcomes with a slim modiolar cochlear implant electrode array. *Otolaryngol Head Neck Surg*. 2020;162:731–6.
- Gabrielpillai J, Burck I, Baumann U, Stöver T, Helbig S. Incidence for tip foldover during cochlear implantation. *Otol Neurotol*. 2018;39:1115–21.
- Grolman W, Maat A, Verdam F, Simis Y, Carelsen B, Freling N, et al. Spread of excitation measurements for the detection of electrode array foldovers: a prospective study comparing 3-dimensional rotational x-ray and intraoperative spread of excitation measurements. *Otol Neurotol*. 2009;30:27–33.
- Hey M, Neben N, Stöver T, Baumann U, Mewes A, Liebscher T, et al. Outcomes for a clinically representative cohort of hearing-impaired adults using the Nucleus® CI532 cochlear implant. *Eur Arch Otorhinolaryngol*. 2020;277:1625–35.
- Hey M, Wesarg T, Mewes A, Helbig S, Hornung J, Lenarz T, et al. Objective, audiological and quality of life measures with the CI532 slim modiolar electrode. *Cochlear Implants Int*. 2019;20:80–90.
- Ishiyama A, Risi F, Boyd P. Potential insertion complications with cochlear implant electrodes. *Cochlear Implants Int*. 2020;21:206–19.

- Jwair S, Prins A, Wegner I, Stokroos RJ, Versnel H, Thomeer HGXM. Scalar translocation comparison between lateral wall and perimodiolar cochlear implant arrays: a meta-analysis. *Laryngoscope*. 2021 Jun;131(6):1358–68.
- Klabbers TM, Huinck WJ, Heutink F, Verbist BM, Mylanus EAM. Transimpedance matrix (TIM) measurement for the detection of intraoperative electrode tip foldover using the slim modiolar electrode: a proof of concept study. *Otol Neurotol*. 2021 Feb 1;42(2):e124–9.
- de Leeuw J, Mair P. Multidimensional Scaling Using Majorization: SMACOF in R. *J Stat Softw*. 2009;31(3):1–30.
- Mittmann P, Lauer G, Ernst A, Mutze S, Hasseplass F, Arndt S, et al. Electrophysiological detection of electrode fold-over in perimodiolar cochlear implant electrode arrays: a multicenter study case series. *Eur Arch Otorhinolaryngol*. 2020;277:31–5.
- Müller A, Kropp MH, Mir-Salim P, Aristeidou A, Dziemba OC. Intraoperative tip-foldover-screening mittels spread of excitation mes-sungen. *Z Med Phys*. 2021 Aug;31(3):276–88.
- Trecca EMC, Adunka OF, Mattingly JK, Hiss MM, Cassano M, Malhotra PS, et al. Electrocochleography observations in a series of cochlear implant electrode tip fold-overs. *Otol Neurotol*. 2021 Apr 1;42(4):e433–7.
- Vanpoucke FJ, Boermans PP, Frijns JH. Assessing the placement of a cochlear electrode array by multidimensional scaling. *IEEE Trans Biomed Eng*. 2012;59:307–10.
- Zuniga MG, Rivas A, Hedley-Williams A, Gifford RH, Dwyer R, Dawant BM, et al. Tip fold-over in cochlear implantation: case series. *Otol Neurotol*. 2017 Feb;38(2):199–206.